[3] Partridge, D. W. and Pecover, B. E., "An Application of the RAE Wind-Tunnel/Flight Dynamics Simulator to the Low Speed Dynamics of a Slender Delta Aircraft (HP 115)," Repts. and Memos. 3669, 1969, Aeronautical Research Council, London, England.

[4] Engler, P. B. E. and Moss, G. F., "Low-Speed Tunnel Tests on a $\frac{1}{8}$th Scale Model of the Handley Page HP 115," Repts. and Memos. 3486, 1965, Aeronautical Research Council, London, England.

[5] Thompson, J. S. and Fail, R. A., "Oscillatory Derivative Measurement on Sting-Mounted Wind-Tunnel Models at RAE Bedford," AGARD Current Paper 17, 1966.

[6] Beecham, L. J. and Titchener, I. M., "Some Notes on an Approximate Solution for the Free Oscillation Characteristics of Nonlinear Systems Typified by $\ddot{x} + F(x,\dot{x}) = 0$," Repts. and Memos. 3651, 1969, Aeronautical Research Council, London, England.

[7] Kryloff, N. and Bogoliuboff, N., *Introduction to Nonlinear Mechanics*, Princeton University Press, Princeton, N.J., 1937.

[8] Ross, A. J. and Beecham, L. J., "An Approximate Analysis of the Nonlinear Lateral Motion of a Slender Aircraft (HP 115) at Low Speeds," Repts. and Memos. 3674, 1971, Aeronautical Research Council, London, England.

[9] Henderson, J. M., "Low Speed Handling of a Slender Delta (HP 115)," *Journal of the Royal Aeronautical Society*, Vol. 69, No. 653, 1965, pp. 311–324.

[10] Thompson, J. S., Fail, R. A., and Inglesby, J. V., "Low Speed Wind-Tunnel Measurements of the Oscillatory Lateral Stability Derivatives for a Model of the Slender Aircraft (HP 115) Including the Effects of Frequency Parameter," Current Paper 1097, 1969, Aeronautical Research Council, London, England.

SEPTEMBER 1972 J. AIRCRAFT VOL. 9, NO. 9

An Improved Solution of the Two-Dimensional Jet-Flapped Airfoil Problem

RICHARD G. LEAMON*
Naval Ordnance Laboratory, White Oak, Md.
AND
ALLEN PLOTKIN†
University of Maryland, College Park, Md.

A method of solution is developed for a two-dimensional jet-flapped airfoil in potential flow. Numerical solutions are obtained which contain the proper singularities and which properly satisfy the boundary conditions on the airfoil and jet surfaces along their actual positions. A discussion of previous work is given. Comparisons of the method with previous work and experimental measurements are made. For momentum coefficients up to 1.0 and initial jet deflection angles of up to 60.0° the present method gives values of the sectional lift and pitching moment coefficients which differ from previous methods—those using the shallow jet approximation—by up to 16% but which lie within the range of experimental results.

I. Introduction

THE jet flap is a high lift device which employs a thin jet of high speed air ejected downward at the trailing edge of an airfoil (Fig. 1). The phenomenon was first extensively investigated by Hagedorn and Ruden.[1] Subsequent tests have produced sectional lift coefficients as high as 10.0. A sketch of the early development of the basic principle and accompanying theory is given in Stafford.[8] High lift coefficients are achieved by using the jet for two reasons: 1) a change in the pressure distribution over the airfoil chord which produces a net increase in the lift and 2) the reaction to the vertical momentum exhausted by the airfoil into the jet.

This paper presents a new method of calculating two-dimensional potential flow about a jet-flapped airfoil. Previous methods, accorded to Spence,[3] Hough,[4] and Malavard,[5] obtain a solution by distributing a singular solution (vortex sheet) along a semi-infinite line parallel to the undisturbed flow and passing through the trailing edge of the airfoil (Fig. 2a). Such a representation is here denoted as the shallow jet approximation. The present method places the singular solution along the mean camber line of the airfoil and the mean position of the jet (Fig. 2b) and, in contrast to these previous methods, satisfies the boundary condition at the actual position of these surfaces. This representation provides more accurate results in the sense of satisfying the boundary conditions more realistically at the cost of considerable mathematical complication. This representation was also used by Herold[6] who constructed a solution using a finite number of discrete vortex filaments placed along the airfoil and jet.

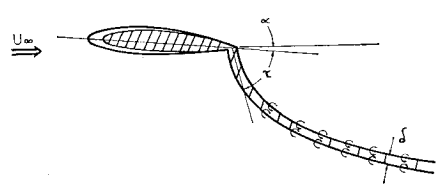

Fig. 1 Jet-flapped airfoil at angle of attack α with initial jet deflection τ.

Received August 27, 1971; revision received April 17, 1972. The computer time for this research was supplied by the Computer Science Center of the University of Maryland. The authors would like to thank H. Snay, W. Melnik, and L. Filotas for their useful suggestions.

Index categories: Subsonic and Transonic Flows; Jets, Wakes, and Viscid-Inviscid Flow Interactions

* Research Physicist.

† Associate Professor of Aerospace Engineering. Member AIAA.

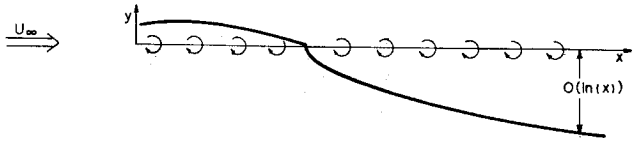

Fig. 2a Location of the singular solution for previous research.[3-5]

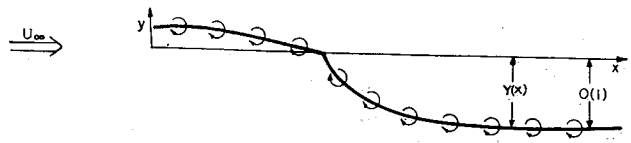

Fig. 2b Location of the singular solution for present research.

II. Analysis

If the airfoil section is thin, and if the jet width is small compared to its radius of curvature, the airfoil and jet may be represented as a single vortex sheet. The velocity component normal to this sheet must vanish and this boundary condition may be used to derive an integral equation for the vortex sheet strength. A solution of this integral equation may be obtained numerically.

A. Thin Jet

The momentum flux of the jet J is a constant because we assume no viscous mixing. Further, we assume a thin jet by letting the jet thickness δ approach zero but requiring J to remain finite.

We define the momentum coefficient C_J, for a jet-flapped airfoil of chord c, in a flow with freestream speed U_∞ and density ρ_∞, to be

$$C_J = J/\tfrac{1}{2}\rho_\infty U_\infty^2 c \tag{1}$$

Then the vorticity along the jet is given by

$$\gamma_j = C_J U_\infty^2 c/2\bar{u}R \tag{2}$$

where $\bar{u}$ is the average of the tangential velocity components just above and below the jet, and R is the radius of curvature of the jet centerline. Full details are given in Spence.[3]

B. Integral Equation

We use the boundary condition that the velocity component normal to the vortex sheet which represents the airfoil and jet must vanish to derive an integral equation for the vortex sheet strength. The total induced velocity at a point located a distance s along the sheet, $\mathbf{q}(s)$, is given by

$$\mathbf{q}(s) = \int_0^\infty \frac{\boldsymbol{\gamma}(s_1) \times \mathbf{r}(s_1,s)}{2\pi|\mathbf{r}(s_1,s)|^2}\, ds_1 \tag{3}$$

where $\boldsymbol{\gamma}(s)$ is the vortex sheet strength with direction parallel to the filaments comprising the sheet, $\mathbf{r}(s_1,s)$ is the vector from s_1 to s, and the integral is taken in the Cauchy principal value sense.

The boundary condition requires the normal component of the sum of the induced and free stream velocities to vanish. If Eq. (2) is also used to express the vortex sheet strength along the jet in terms of R, the desired integral equation becomes

$$\int_0^c [\boldsymbol{\gamma}_f(s_1) \times \mathbf{r}(s_1,s)] \cdot \hat{n}(s) ds_1 / 2\pi|\mathbf{r}(s_1,s)|^2 + \int_c^\infty \frac{[C_J|\mathbf{U}_\infty|^2 c\hat{v}(s_1) \times \mathbf{r}(s_1,s)] \cdot \hat{n}(s)\, ds_1}{4\pi R(s_1)|\mathbf{r}(s_1,s)|^2 |[\mathbf{U}_\infty + \mathbf{q}(s_1)] \times \hat{n}(s)|} + \mathbf{U}_\infty \cdot \hat{n}(s) = 0 \tag{4}$$

where $\hat{v}(s)$ and $\hat{n}(s)$ are unit vectors parallel and normal to the vortex sheet, respectively, and $\boldsymbol{\gamma}_f$ is the vorticity along the airfoil. A solution is obtained when $\boldsymbol{\gamma}_f$ and a jet shape $R(s)$ are found which satisfy Eq. (4) at every point s along the vortex sheet.

No approximations are required to obtain a numerical solution of Eq. (4) using the method presented here. However, solutions have been obtained by several researchers[3-5] using an approximate form of Eq. (4). First, these researchers approximate the boundary condition by applying it along a line parallel to the freestream velocity and passing through the trailing edge of the airfoil (cf. Fig. 2a). For the airfoil section this approximation is usually made for thin airfoils and implies that the airfoil mean camber line lies close to the x axis of Fig. 2a. For the thin jet such an approximation may be termed the shallow jet approximation and implies that the thin jet also lies close to the x axis. The singular solutions used to represent the airfoil and jet are also placed along the x axis as is shown in Fig. 2a. Concurrent with the physical approximation of the shallow jet, a mathematical approximation is made. As the shallow jet approximation holds only for thin jets lying close to the x axis of Fig. 2a, it is argued that the first derivative of the jet center line function $Y(x)$ (see Fig. 2b) is small. Thus the curvature is approximated by the second derivative of $Y(x)$. Table 1 shows the accuracy of this approximation when used to determine the vorticity of several jet center line shapes shown in Fig. 6. Spence[3] obtains a numerical solution of the Eq. (4) for a flat plate, jet-flapped airfoil under these assumptions. Hough,[4] using a roughly similar approach, examined the case of a cambered jet-flapped airfoil. Malavard[5] examined the flat plate, jet-flapped airfoil under these assumptions using a rheoelectric analogue. An interesting artifact of the approach used first by Spence[3] is the asymptotic downstream behavior of the jet center line shape, namely,

$$\lim_{x\to\infty} Y(x) \to 0[\ln(x)]$$

Such a condition would mean that streamlines at downstream infinity would display infinite displacements. However, this anomaly does not seem to have computational importance.

Herold[6] obtained a numerical solution of Eq. (4) for the flat plate, jet-flapped airfoil using discrete vortex filaments without recourse to the shallow jet approximations. The jet is represented by several straight line segments. He takes no special account of the singularities in the vorticity at the

Table 1 Accuracy of the shallow jet approximation

	x/c	γ_J[Eq. (2)][a,b]	γ_J(shallow jet)	$C_J c/2R$
	1.1	0.1441	0.1449	0.1436
$\alpha = 0.0°$	1.5	0.06311	0.06333	0.06300
$\tau = 5.0°$	2.0	0.03800	0.03809	0.0796
$C_J = 4.0$	3.0	0.02244	0.02246	0.02243
	5.0	0.01137	0.01138	0.01137
	10.0	0.002005	0.002005	0.002005
	1.1	0.9377	1.198	0.8295
$\alpha = 0.0°$	1.5	0.3800	0.4367	0.3544
$\tau = 31.4°$	2.0	0.2041	0.2237	0.1950
$C_J = 4.0$	3.0	0.1141	0.1201	0.1112
	5.0	0.06981	0.07115	0.06915
	10.0	0.01976	0.01978	0.01975
	1.1	1.655	13.96	0.5703
$\alpha = 0.0°$	1.5	1.108	3.139	0.6584
$\tau = 75.0°$	2.0	0.4498	0.8433	0.3285
$C_J = 4.0$	3.0	0.2523	0.3727	0.2076
	5.0	0.2270	0.2575	0.2132
	10.0	0.04322	0.04337	0.04315

[a] Vorticity strengths are based on the jet center line positions shown in Fig. 9.
[b] $U_\infty = 1$.

leading and trailing edges, or of the leading edge suction. This approach seems limited in its ability to specify the downstream asymptotic position of the jet center line.

C. Assumed Form of the Solution

In order for Eq. (4) to be solved numerically by the method described here, it is necessary to assume closed form analytic expressions for the airfoil vorticity γ_f, and the jet centerline position Y. Far from arbitrary these expressions must display several properties which are dictated by special considerations of the problem. Further, such expressions must contain as few optimization parameters as possible in the interest of saving computational effort.

The vortex sheet strength representing the thin airfoil must have a singularity of $0(x^{-1/2})$ as $x \to 0$ at the leading edge.[9] In addition a singularity of $0[\ln(x-c)]$ as $x \to c$ is necessary at the trailing edge.[10] With these considerations taken into account, the assumed form of the airfoil vorticity is taken as

$$\gamma_f(x) = ax^{-3/2}\ln(1-x) + A_1 x \ln(1-x) + A_2 x(1-x)^2 \quad (5)$$

where x is taken as the x axis of Fig. 2b, and the airfoil chord is taken as unity. The authors feel that this distribution should adequately describe airfoils whose camber falls within the limitations of thin-airfoil theory but at this time have only investigated the flat plate case. A constitutive relation for "a" may be derived by consideration of the leading edge suction force, S. This suction force in terms of the vorticity representing the airfoil is given by[9]

$$S = (\pi/4)\rho_\infty[\lim_{x\to 0} x^{1/2}\gamma_f(x)]$$

and acts tangent to the camber line at the leading edge. For the flat plate, this becomes

$$a^2 = \frac{4}{\pi\rho_\infty}(\{J[1-\cos(\tau+\alpha)] + \rho_\infty \int_0^c \gamma_f(s)[\mathbf{U}_\infty + \mathbf{q}(s)]\cdot\hat{n}(s)\, ds\}/\cos\alpha) \quad (6)$$

where α is the airfoil angle of attack and τ is the initial jet deflection angle as shown in Fig. 1.

As in the case of the airfoil, the vortex sheet strength representing the jet center line must have the singularity of $0[\ln(x-c)]$ as $x \to c^+$ at the trailing edge, which means that $\lim |Y''(x)| \to 0[\ln(x-c)]$. Also $Y(x)$ must be tangent to the initial jet deflection angle, τ, at the trailing edge which means $\lim Y'(x) = \tan(\alpha+\tau)$ (x is the x axis of Fig. 2b). Such a function $Y(x)$ can be constructed from two terms $y_1(x)$ and $y_2(x)$.

Consider first $y_1(x)$ given as

$$y_1(x) = (x-1)^2\ln(x-1)/2 - x^2\ln x/2 + x\ln x + (x-1)/2$$

where c has again been taken as unity. Note that $y_1(1) = 0$, $y_1'(1) = 1$, and $y_1'(x) = 0[\ln(x-1)]$ as $x \to 1^+$ as was desired. In order that the jet center line position have a finite displacement at downstream infinity, $y_1(x)$ must be combined with $y_2(x)$ given as

$$y_2(x) = B(1 - e^{-\varepsilon_2(x-1)})$$

Now $Y(x)$ may be written as

$$Y(x) = by_1(x)e^{-\varepsilon_1(x-1)} + y_2(x) \quad (7)$$

where $b = \tan(\alpha+\tau) - y_2'(1)$. Note that far downstream $Y(x) \to B$ as was desired, and for small ε_2, Eq. (7) gives a reasonable approximation of Spence's[3] solutions.

E. Numerical Methods

A scheme which iterates upon the parameters for the airfoil vorticity and the jet center line position may be employed to satisfy Eq. (4) at several points along the airfoil and the jet.

Initial estimates of the airfoil vorticity (a, A_1, and A_2) and the jet center line parameters (B, ε_1, and ε_2) are made. Several points at which Eq. (4) is to be satisfied are selected. Equation (4) evaluated at these points may be viewed as a system of nonlinear equations where the parameters are the independent variables. Equation (6) also becomes part of this system. At each iteration of the parameters Eq. (3) must be used in a subiteration to determine $\mathbf{q}$—note that $\mathbf{q}$ appears under the integral on the RHS of Eq. (3) for the portion of the integration where $\gamma = \gamma_f$—as $\mathbf{q}$ appears on the RHS of Eq. (4). Multidimensional Newton-Raphson iteration is used to solve this system. Partial derivatives with respect to the parameters are obtained numerically. This scheme further can be made to allow the system to be over-specified (i.e., more points may be considered than parameters) in which case Eq. (4) is satisfied at the points in the least-squares sense.

To obtain the numerical results shown in Figs. 3–9, 6–10 points were chosen along the airfoil and jet. Typically these points were at 0.2, 0.5, 0.8, 1.2, 1.5, 2.0, 5.0, 7.0, and 15.0 ($c = 1.0$). As long as the points were not all clustered in one location, their exact position makes no significant difference. Iteration was continued until Eq. (4) was satisfied to within 0.001 U_∞ at each point. With reasonable initial parameters the iteration required 6–8 min of IBM 7094 IBSYS computer time. The value of $\mathbf{q} \times \hat{n}(s)$ was found to be small compared to $\mathbf{U}_\infty \times \hat{n}(s)$ for all cases shown here and could be ignored to attain some saving of computer time.

The numerical integration formulas used were of the gauss type. Special considerations were required at the leading and trailing edges where the vorticity is singular, and in obtaining the Cauchy principal value when $s = s_1$ in Eqs. (3) and (4). Laguerre integration was used in the integration to downstream infinity. Several checks of the numerical integration scheme were made. Details of the numerical methods employed may be found in Ref. 7.

III. Comparison with Experiments and Other Methods

The method described here was used to obtain numerical results for a flat plate jet-flapped airfoil. The method is in no way limited to an uncambered airfoil, but the flat plate illustrates all the essential features of the jet flap yet affords a modest mathematical simplification. Other theoretical methods and experimental results are available for comparison.

The theoretical work of others[3–6] has been discussed. Experimental results due to Dimmock[11] and Malavard et al.[12] are also available. Dimmock tested a jet-flapped airfoil of elliptical cross section with 15% thickness and an 8-in. chord. Malavard et al. tested a NACA 0018 jet-flapped airfoil with a chord of about 1 ft. For both tests the Reynolds number based on the airfoil chord was $1-6\times10^5$. In reducing Dimmock's results for presentation here the pitching moment about an elliptical cylinder in potential flow was subtracted

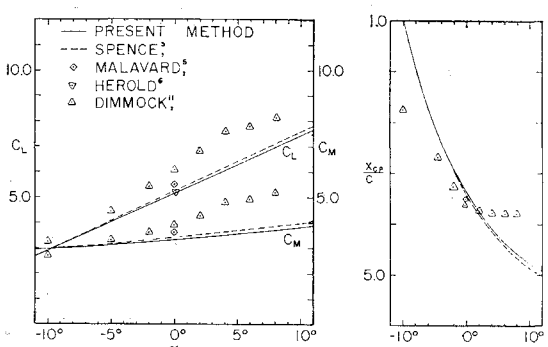

Fig. 3 Aerodynamic coefficients vs α; $\tau = 31.4°$, $C_J = 4.0$.

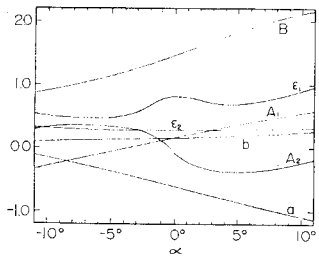

Fig. 4 Plate vorticity and jet center line position parameters vs α; $\tau = 31.4°$, $C_J = 4.0$.

from the observed pitching moments. The potential flow thickness correction of Spence[3] was not applied to Dimmock's data because of its approximate nature. In reducing the data of Malavard et al the finite aspect ratio correction of Hartunian[2] was applied using the aspect ratio of 20 given by these researchers.

Figures 3–6 present results for the case $C_J = 4.0$. This is the case examined in greatest detail by Spence. Figure 3 shows the variation in C_L, C_M, and x_{cp} (from now on referred to as the aerodynamic coefficients) as they are defined in Spence and discussed fully in Ref. 7, with α for $C_J = 4.0$ and $\tau = 31.4°$. For these coefficients agreement is excellent with the results of Spence,[3] Malavard,[5] and Herold[6] (1.4%, 6%, and 0.5%, respectively). There are slight differences, less than 4%, in $\partial C_L/\partial\alpha$ and $\partial C_M/\partial\alpha$ with Spence's results. Agreement between these theoretical methods and Dimmock's[11] measurements is not good. However, he reports leading edge boundary-layer separation for $\alpha > -3°$. Agreement between the present method and his measurements is approximately 10% for $\alpha < -3°$. Stall appears to occur for $\alpha > 5°$ in his tests. Figure 4 shows the parameters of Eqs. (5) and (7) for this case.

Figure 5 shows the variation in the aerodynamic coefficients with τ for $C_J = 4.0$ and $\alpha = 0.0°$. For small τ the shallow jet approximation becomes valid and the present method merges into those of Spence[3] and Malavard.[5] The experimental points of Dimmock[11] were reported to suffer leading edge separation. Figure 6 shows the position of the jet center line for several values of τ with $C_L = 4.0$ and $\alpha = 0.0$. As expected great differences are seen for large τ between the present method and that of Spence.[3] Note that for the downstream distances shown, the asymptotic behavior of Spence's $Y(x)$ has not caused his results to diverge from ours, except for $\tau = 5°$. Further downstream Spence's $Y(x)$ will cross that of the present method.

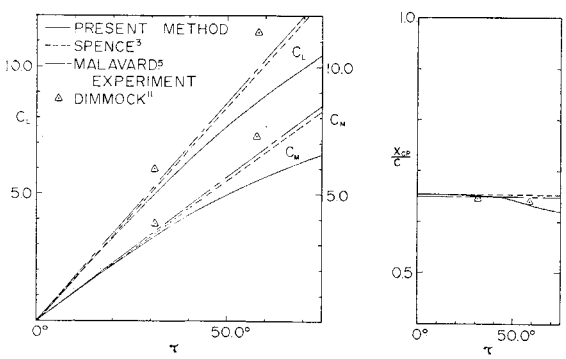

Fig. 5 Aerodynamic coefficients vs τ; $\alpha = 0.0°$, $C_J = 4.0$.

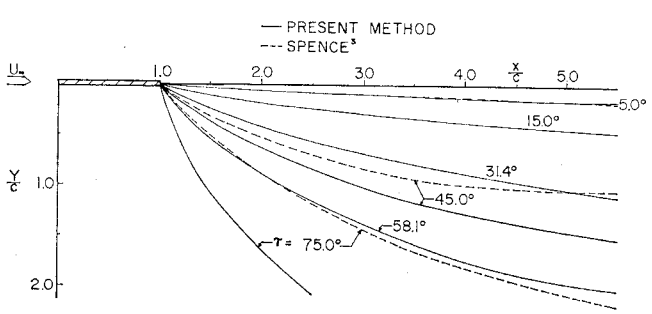

Fig. 6 Position of jet center line for several τ's; $\alpha = 0.0°$, $C_J = 4.0$.

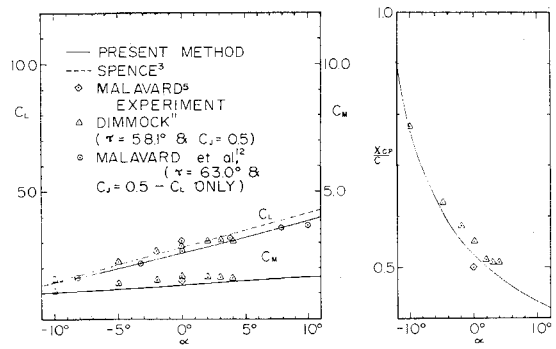

Fig. 7 Aerodynamic coefficients vs α; $\tau = 60.0°$, $C_J = 0.5$.

Figure 7 shows the variation in the aerodynamic coefficients with α for $C_J = 0.5$ and $\tau = 60.0°$. Agreement with the results of Spence[3] and Malavard[5] is within 8% even for such a high value of τ. There is a difference of 10% in $\partial C_L/\partial\alpha$ between the present method and Spence. Agreement with the experiments of Malavard et al.[12] ($\tau = 63.0°$) is better than 2% and agreement with Dimmock's[11] measurements ($\tau = 58.1°$) is within 16%. Dimmock reports leading edge separation for $\alpha > 0°$, and stall appears to occur for $\alpha > 2°$. Stall occurs for $\alpha > 8°$ in the test of Malavard et al. and no leading edge separation is reported.

Figure 8 shows the variation in the aerodynamic coefficients with α for $C_J = 1.0$ and $\tau = 57.3°$. Agreement with the results of Spence[3] and Malavard[5] is 16%. Agreement of C_L with the measurements of Malavard et al. ($C_J = 0.9$, $\tau = 55.0°$) is better than 3%; agreement with their C_M measurements is 63%. However, they are not corrected for pressures acting parallel to the chord. Stall appears for $\alpha > 8°$. Dimmock ($C_J = 1.0$, $\tau = 58.1°$) reports leading edge separation for $\alpha > -5°$ and stall occurs for a $\alpha > 1°$. Agreement with Dimmock's measurements is within 5% for $\alpha < -5°$.

Figure 9 shows the excellent agreement between Dimmock's measurements and the jet center line position function for $\alpha = 0.0°$, $C_J = 1.0$, and $\tau = 31.4°$. Results are also given for the aerodynamic coefficients. Agreement between the present method and those of Spence[3] and Malavard[5] for the coefficients is within 8%. Agreement with the results of Herold[6] for C_L is only 28%. Agreement with Dimmock's measurements is 17%.

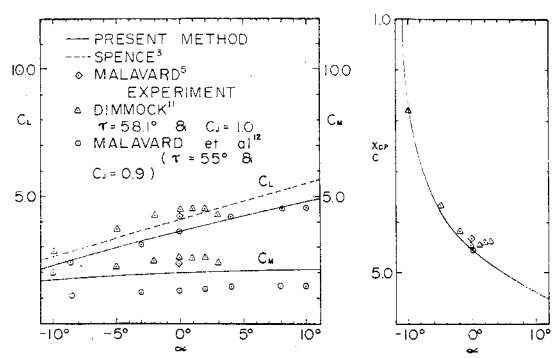

Fig. 8 Aerodynamic coefficients vs α; $\tau = 57.3°$, $C_J = 1.0$.

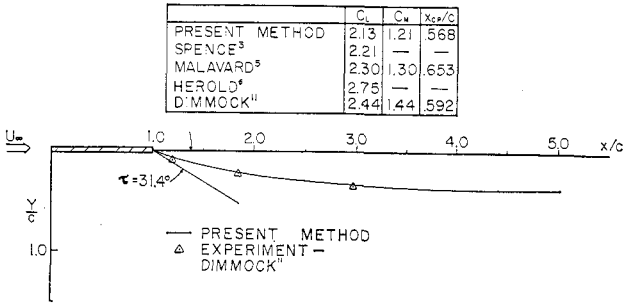

Fig. 9 Aerodynamic coefficients and position of jet center line; $\alpha = 0.0°$, $\tau = 31.4°$, $C_J = 1.0$.

IV. Conclusions and Recommendations

Agreement between the present study and the work of Spence[3] and Malavard[5] for C_L, C_M, and x_{cp} is within 16% for C_J up to 1.0 and τ up to 60.0°. Major differences, more than 20%, between the present method and the work of these researchers are seen only for large values of C_J and τ, e.g., $C_J = 4.0$, $\tau > 70.0°$. The agreement with Herold[6] of 6% for $\alpha = 0.0°$, $C_J = 4.0$, $\tau = 31.4°$ and 28% for $\alpha = 0.0°$, $C_J = 1.0$, $\tau = 31.4°$ is the reverse of what should be expected (i.e., agreement should be better both with the present method and shallow jet methods for smaller C_J). This points up the need for further refinement of the discrete vortex filament approach-probably a need exists to take particular account of the vorticity singularities at the leading and trailing edges as well as the downstream asymptotic position of the jet.

Agreement between the present method and experimental measurements is good—all things considered. Agreement of C_L, C_M, and x_{cp} as compared with the measurements of Dimmock[11] is within 17% for those observations made when the ellipse was unstalled and displayed no leading edge separation. Agreement with Malavard et al.[12] for values of C_L is better than 3% for unstalled observations. It would appear that the more streamlined shape of the NACA 0018 airfoil helped alleviate the leading edge separation. Agreement with their observation of C_M is poor but this is probably due to pressure forces acting across the thickness of the section so as to turn it parallel to the free stream. It is unfortunate that no such correction was applied to their data.

It may be concluded that the method described here gives at least as good predictions of C_L, C_M, and x_{cp} for a thin jet-flapped airfoil as the shallow jet approximation. In contrast to the work of Herold,[6] the method merges smoothly into the limiting case of the shallow jet. The method appears to give the best prediction of these coefficients for streamlined airfoil sections; however, additional experiments using the thinnest possible airfoil section are required to determine clear cut superiority of any one method.

Numerical results for the cambered thin-jet-flapped airfoil may be easily obtained using the present method. These results could be compared with the shallow jet work of Hough.[4] The general approach of the method is applicable to finding numerical solutions of any potential flow boundary-value problem where the position of part of the boundary is a function of the solution.

References

[1] Hagerdorn, H. and Ruden, P., "Windkanaluntersuchungen an einem Junkers-Doppelflugel mit Ausblaseschlitz am Heck des Hauptflugels," Institut Fur Aeromechanik und Flugtechnik der Technischen Hochschule Hannover, *LGL Bericht A64*, 1938, pp. 38–56; also R.A.E. translation 442, Dec. 1953.

[2] Hartunian, R.A., "The Finite Aspect Ratio Jet Flap," Rept. A1-1190-A-3, Oct. 1959, Cornell Aeronautical Lab., Buffalo, N. Y.

[3] Spence, D.A., "The Lift Coefficient of a Thin Jet Flapped Wing," *Proceedings of the Royal Society, Series A*, Vol. 238, No. 1212, Dec. 1956, pp. 46–68.

[4] Hough, G.R., "Cambered Jet-Flapped Airfoil Theory," M.S. thesis, Sept. 1959, Cornell Univ., Ithaca, N.Y.

[5] Malavard, L.E., "Recent Developments in the Method of the Rheoelectric Analogy Applied to Aerodynamics," *Journal of the Aeronautical Sciences*, Vol. 24, No. 5, May 1957, pp. 321–331; also Revuz, J., *Etude analogique du soufflage au bord de futie d'un profil d'aide, Proceedings of the International Analogy Computation Meeting*, Bruxells, Oct. 1955.

[6] Herold, A.C., "A Two-Dimensional, Iterative Solution for the Jet Flap," M.S. thesis, Nov. 1969, Univ. of Washington, Seattle, Wash.

[7] Leamon, R.G., "An Improved Solution of the Two-Dimensional Jet-Flapped Airfoil Problem," M.S. thesis, Aug. 1971, Univ. of Maryland College Park, Md.

[8] Stafford, B.S., "Early Thoughts on the Jet Flap," *The Aeronautical Quarterly*, Vol. VII, Oct. 1955, pp. 45–59.

[9] von Karman, J. and Burgers, J.M., "General Aerodynamic Theory—Perfect Fluids," *Aerodynamic Theory*, edited by W.F. Durand, Dover, New York, 1935, pp. 48–56.

[10] Landahl, M., "Pressure-Loading for Oscillating Wings with Control Surfaces," *AIAA Journal*, Vol. 6, No. 2, Feb. 1968, pp. 345–348; also Glauert, H., "Theoretical Relationships for an Airfoil with Hinged Flaps," Rept. No. 1095, April 1927, Aeronautical Research Committee, London, England.

[11] Dimmock, N.A., "An Experimental Introduction to the Jet Flap," and "Some Further Jet Flap Experiments," Current Papers 344 and 345, Oct. 1957, Aeronautical Research Council, London, England; also Dimmock, N.A., "Some Early Jet Flap Experiments," *The Aeronautical Quarterly*, Vol. VIII, No. 4, Nov. 1957, pp. 331–345.

[12] Malavard, L., Poisson-Quinton, P., and Jousserandot, P., "Jet Induced Circulation Control: Part II Experimental Results," *Aero Digest*, Vol. 73, No. 4, Oct. 1956, pp. 46–59.